Computational Dispersion Properties of Vertically Staggered Grids for Atmospheric Models

MICHAEL S. FOX-RABINOVITZ*

Laboratory for Atmospheres, NASA/Goddard Space Flight Center, Greenbelt, Maryland

(Manuscript received 25 May 1993, in final form 27 August 1993)

ABSTRACT

The computational dispersion properties of vertically and time-vertically staggered grids, using corresponding centered-difference schemes for approximation of a linear baroclinic primitive equation system, are analyzed in terms of frequency and group velocity characteristics. The vertical scale ranges with group velocities of the wrong sign are pointed out.

It is shown that among all possible vertical grids applicable to primitive equation atmospheric models the best vertical grids have computational dispersion properties corresponding to a regular (equidistant, unstaggered) grid with *twice* the vertical resolution. These best vertical grids are 1) two well-known vertically staggered grids, namely, the widely used Lorenz grid and the Charney–Phillips grid; 2) two other vertically staggered grids carrying both horizontal and vertical velocity components at the same levels; and 3) the new time-staggered versions of all the aforementioned grids, and the time-staggered regular vertical grid, if used with either the appropriate version of an economical explicit scheme or a semi-implicit scheme for approximations with these time-staggered grids. All these best vertical grids are computationally efficient due to their enhanced effective vertical resolution.

Moreover, the time-vertically staggered grids considered here provide twice the effective vertical resolution of comparable vertically staggered grids for finite-difference approximations of the vertical derivatives in vertical advection and vertical diffusion terms. In other words, these time-vertically staggered grids provide uniformly twice the effective vertical resolution for the whole baroclinic model system.

The application of higher- (fourth) order vertical-difference approximation results in some moderate improvement of vertical grid dispersion properties, primarily for the small vertical and large horizontal scale range, but it is definitely less significant than the effect of doubling the effective vertical resolution by staggering.

Computational dispersion properties of vertical grids, along with other computational characteristics and requirements, may provide guidance for an optimal choice of an appropriate vertical grid for a primitive equation atmospheric model.

1. Introduction

Horizontally and vertically staggered grids are widely used in atmospheric models. The best grids of this kind provide better effective spatial resolution, at least for the adjustment terms. An example of a horizontally staggered grid is the Arakawa C grid widely used in atmospheric models (e.g., Mesinger and Arakawa 1976). Another kind of staggered grid is the Eliassen grid, which is staggered in the horizontal and in time (e.g., Eliassen 1956; Mesinger and Arakawa 1976). When studying the computational properties of these grids, the corresponding central difference schemes (CDS) are usually used. Along with investigating the computational stability properties, the study of the computational dispersion properties of these grids together with their corresponding CDSs has been found to be very important (e.g., Roache 1976; Mesinger and Arakawa 1976; Grotjahn and O'Brien 1976; Neta and Williams 1986; Wajsowicz 1986; Neta and Navon 1989; Neta and Williams 1989a,b). Specifically, the advantages of analyzing group velocity properties have been shown in many studies (e.g., Grotjahn and O'Brien 1976; Schoenstadt 1980; Trefethen 1982; Vichnevetsky and Bowles 1982; Fox-Rabinovitz 1988; Neta and Williams 1989a). A complete analysis of the computational dispersion properties of practically all possible horizontally and time horizontally staggered grids is presented in Fox-Rabinovitz (1991a).

The study of appropriate vertical grids for atmospheric models began from the pioneering works of Charney and Phillips (1953) and Lorenz (1960). It was continued by others (e.g., Tokioka 1978) and especially by Arakawa and his collaborators (e.g., Arakawa 1984; Arakawa and Suarez 1983; Arakawa and Moorthi 1988).

* Current affiliation: Universities Space Research Association.

Corresponding author address: Dr. Michael S. Fox-Rabinovitz, Laboratory for Atmospheres, Code 910.3, NASA/Goddard Space Flight Center, Greenbelt, MD 20771.

The most widely used vertical grid in atmospheric models is the Lorenz (1960) staggered grid, or the L grid, which carries the horizontal velocities and temperatures at the same levels, and vertical velocities at the intermediate levels (Fig. 1). The advantage of the Lorenz grid lies in its easy maintenance of conservation laws. The Charney–Phillips (1953) staggered grid, or the CP grid, carries vertical velocities and temperatures at the same levels, and horizontal velocities at the intermediate levels (Fig. 1). The advantage of this grid is in its easy maintenance of integral constraints for a quasigeostrophic flow, such as the conservation of quasigeostrophic potential vorticity through horizontal advection. These two vertically staggered grids were compared in a quasigeostrophic system for a baroclinic instability problem by Arakawa and Moorthi (1988), who found that the CP grid controls noise better for relatively small-scale waves than the L grid.

Two new grids (Fig. 1), namely, the time-staggered versions of these vertically staggered grids—that is, the time-staggered L grid, or the LTS grid, and the time-staggered CP grid, or the CPTS grid—have been introduced and preliminarily analyzed in Fox-Rabinovitz (1991b).

This study presents a complete comparative analysis or survey of the computational dispersion properties of practically all possible vertically and time-vertically staggered grids applicable to primitive equation atmospheric models.

It is found out, as a result of the study, that for model adjustment terms not only the well-known vertically staggered L and CP grids but also the new time-verti-

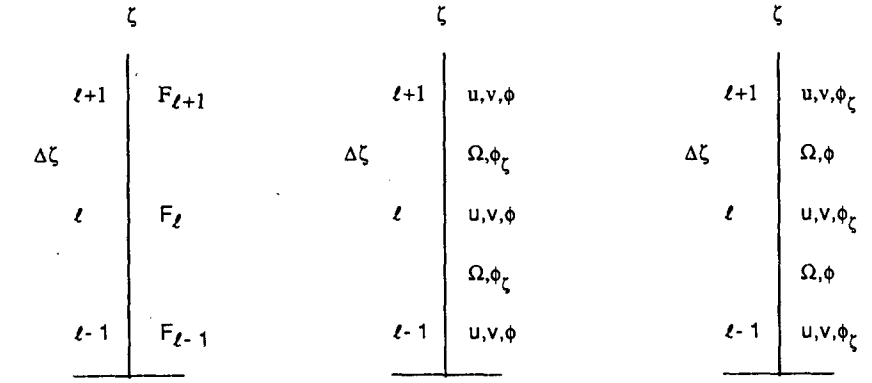

A regular (unstaggered) vertical grid. F-model variables

The vertically staggered Charney-Phillips (CP) grid

The vertically staggered Lorenz (L) grid

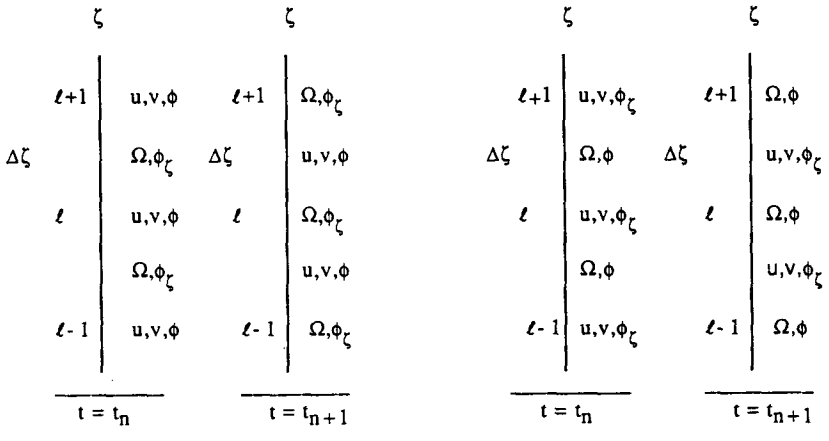

The time-vertically staggered CP grid, or the CPTS grid

The time-vertically staggered L grid, or the LTS grid

FIG. 1. The regular (unstaggered, equidistant) vertical grid, the vertically staggered Charney–Phillips and Lorenz grids, and their time-vertically staggered versions (the CPTS and the LTS grids) (ℓ is a vertical index, $\Delta\zeta$ is a vertical grid increment).

cally staggered grids, when combined with the appropriate time-differencing schemes, provide same advantageous computational dispersion properties corresponding to an unstaggered grid with doubled vertical resolution. Moreover, these new grids provide twice the effective vertical resolution for vertical advection and diffusion terms of a full baroclinic model.

The dispersion equations and the corresponding expressions for the frequency and horizontal and vertical components of group velocity for a linear baroclinic adjustment, or a gravity–inertial wave system for the differential case, are presented in section 2. The corresponding characteristics for centered finite-difference approximations with vertically and time-vertically staggered grids are presented in section 3. The discussion of computational dispersion properties of all considered vertical grids for primitive equation atmospheric models is provided in section 4, and concluding remarks are given in section 5.

2. The differential case

In this section we derive the dispersion characteristics for the gravity–inertial wave system in differential form. In the next section we use them for comparisons with those derived for the discrete systems obtained with different vertically and time-vertically staggered grids.

Let us consider the following linear baroclinic adjustment or wave system in the hydrostatic approximation in a $\zeta = \ln p$ coordinate system:

$$\frac{\partial u}{\partial t} + \frac{\partial \phi}{\partial x} - fv = 0,$$

$$\frac{\partial v}{\partial t} + \frac{\partial \phi}{\partial y} + fu = 0,$$

$$\frac{\partial^2 \phi}{\partial t \partial \zeta} + c^2 \Omega = 0,$$

$$\frac{\partial u}{\partial x} + \frac{\partial v}{\partial y} + \frac{\partial \Omega}{\partial \zeta} = 0, \qquad (1)$$

where u, v, and $\Omega = d\zeta/dt$ are velocity components, c^2 is a constant, ϕ is the geopotential, and f is the constant Coriolis parameter.

The system (1) is the basic one for primitive equation models in p-type coordinate systems.

The solution for the system (1) has the form

$$F = \bar{F} \exp[i(kx + my + r\zeta - \nu t)], \qquad (2)$$

where $k = 2\pi/L_x$, $m = 2\pi/L_y$, $r = 2\pi/L_\zeta$, and L_x, L_y, and L_ζ are wave numbers and wavelengths in the x, y, and ζ directions, respectively, and ν is frequency.

Substituting (2) into (1) we obtain the dispersion equation

$$\nu = f\left\{1 + \lambda^2\left[\left(\frac{k}{r}\right)^2 + \left(\frac{m}{r}\right)^2\right]\right\}^{1/2}, \qquad (3)$$

or for $k = m$,

$$\nu = fA, \qquad (4)$$

where $A = (1 + 2\lambda^2 k^2 r^{-2})^{1/2}$. Here, $\lambda^2 = c^2/f^2$ is the Rossby radius of deformation. Notice that for the considered hydrostatic system (1) the frequency ν in (3) depends on the ratios of the horizontal to vertical wavenumbers, k/r and m/r. It is clear that for the differential problem (1) the horizontal group velocity component (HGVC) is positive and the vertical group velocity component (VGVC) is negative since it follows from (4) that

$$\text{HGVC} = \frac{\partial \nu}{\partial \kappa} = \frac{2f\lambda^2 k r^{-2}}{A} > 0,$$

$$\text{VGVC} = \frac{\partial \nu}{\partial r} = -\frac{2f\lambda^2 k^2 r^{-3}}{A} < 0. \qquad (5)$$

Note that the dispersion characteristics (4) and (5) and the similar ones for the discrete systems we will be examining later are determined only for wavenumbers $r \geqslant r^* = 2\pi/L^*$, where L^* is the vertical scale corresponding to the Brunt–Väisälä oscillation. In general, for the hydrostatic approximation we must have $\nu \geqslant N$, where N is the Brunt–Väisälä frequency.

The characteristics (4) and (5) are used herein for evaluation and comparisons of different grid dispersion properties. Note that the most important criterion used for grid evaluation is that the group velocity components (5) be of the correct sign.

3. Vertically and time-vertically staggered grids

The same dispersion characteristics that were derived for the differential case in the previous section are presented in the following for the system (1) approximated with a CDS for a regular vertical grid and for various vertically and time-vertically staggered grids. The characteristics are compared with each other and against those of the differential case (4) and (5). For simplicity, one of the horizontal grids with the best computational dispersion properties (Fox-Rabinovitz 1991b), namely, the Eliassen grid that provides twice the effective horizontal resolution compared to a regular grid, has been used for all horizontal approximations in the system (1). Note that the most widely used Arakawa C grid has practically the same computational dispersion characteristics, and all results obtained below can be equally applied with that grid as well. The vertical grids to be considered are presented in Figs. 1 and 2. Namely, the regular (unstaggered) vertical grid, the vertically staggered Charney–Phillips (1953) and Lorenz (1960) grids, and two more vertically staggered grids, as well as time-staggered versions of all the aforementioned grids, have been considered. In this way all possible vertically and time vertically staggered grids applicable to atmospheric models are

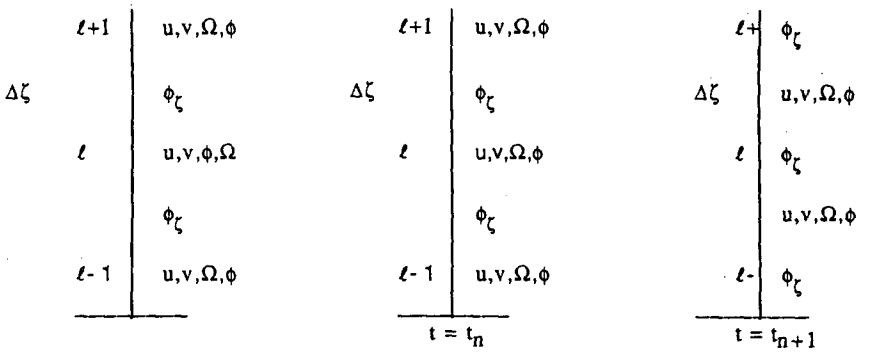

The vertical staggered N1 grid.

The time-vertically staggered N1 grid, or the N1TS grid.

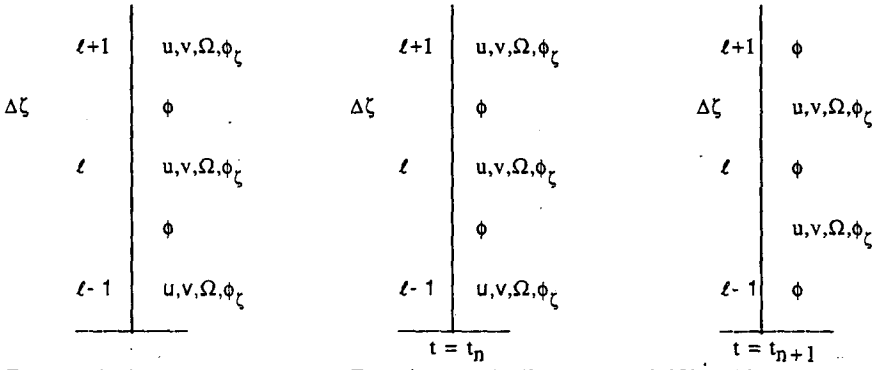

The vertical staggered N2 grid.

The time-vertically staggered N2 grid, or the N2TS grid.

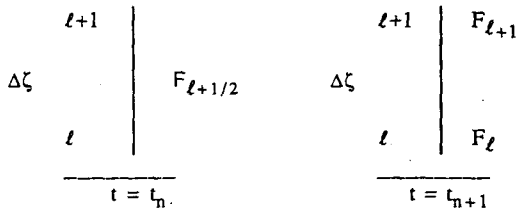

The time-staggered and vertically unstaggered N3TS grid. F-model variables.

FIG. 2. The vertically staggered grids N1 and N2 and their time-vertically staggered versions (the N1TS and the N2TS grids) all carrying horizontal and vertical velocity components at the same levels, and the time-staggered regular (vertically unstaggered) grid (the N3TS grid).

presented and their computational dispersion properties analyzed. Note that the two time-level versions of the semi-implicit (e.g., Robert 1969; Bates 1984) or economical explicit (Shuman 1971; Brown and Campana 1978; Fox-Rabinovitz 1974) schemes may be easily implemented with time-vertically staggered grids. It is important also to notice for practical applications of time-vertically staggered grids that the upper and lower levels for time-vertically staggered grids may be the same for the adjacent time steps. This is very convenient for the incorporation of orography, surface balance, boundary-layer parameterizations, upper-boundary condition formulations, etc.

a. The second-order central-difference scheme for a regular grid

Let us first consider the second-order CDS, or the CDS-2, for the system (1) for the regular (unstaggered, equidistant) vertical grid (Fig. 1) and the Eliassen horizontal grid:

$$\begin{aligned} \bar{u}^t_t + \phi_x - fv &= 0, \\ \bar{v}^t_t + \phi_y + fu &= 0, \\ \bar{\phi}^{t\zeta}_{\bar{t}} + c^2\Omega &= 0, \\ u_x + v_y + \bar{\Omega}^{\zeta}_{\zeta} &= 0, \end{aligned} \tag{6}$$

where differencing and averaging operators used here and in the following are

$$F_z = \frac{1}{\Delta z}\left[F\left(z+\frac{\Delta z}{2}\right) - F\left(z-\frac{\Delta z}{2}\right)\right],$$

$$\bar{F}^z = \frac{1}{2}\left[F\left(z+\frac{\Delta z}{2}\right) + F\left(z-\frac{\Delta z}{2}\right)\right],$$

$$\bar{F}^z_z = \frac{1}{2\Delta z}[F(z+\Delta z) - F(z-\Delta z)],$$

$$\tilde{F}^z = \frac{1}{2}[F(z+\Delta z) + F(z-\Delta z)],$$

$$F_{zz} = \frac{1}{(\Delta z)^2}[F(z+\Delta z) - 2F(z) + F(z-\Delta z)],$$

$$\tilde{F}^{zz} = \frac{1}{4}[F(z+\Delta z) + 2F(z) + F(z-\Delta z)],$$

$$\tilde{F}_{zz} = \frac{1}{(\Delta z/2)^2}\left[F\left(z+\frac{\Delta z}{2}\right) - 2F(z) + F\left(z-\frac{\Delta z}{2}\right)\right], \quad (7)$$

where z is x, y, ζ, or t. We assume that the solution for the finite-difference system (6) has the form

$$F = \hat{F}\exp(k\kappa\Delta x + m\mu\Delta y + r\rho\Delta\zeta - n\nu\Delta t), \quad (8)$$

where κ, μ, ρ, and n are positive numbers.

We assume for simplicity that $k = m$ everywhere below because it will not restrict our basic discussion of computational dispersion properties of vertical grids.

Substituting (8) into (6) and assuming that $\nu\Delta t \to 0$ yields

$$\nu_{\text{CDS-2}} = fB, \quad \text{where}$$

$$B = \left\{1 + 2\lambda^2\left[\frac{\sin(k\Delta x/2)}{\Delta x/2}\right]^2\left(\frac{\sin r\Delta\zeta}{\Delta\zeta}\right)^{-2}\right\}^{1/2}. \quad (9)$$

Now we can derive from (9) the horizontal and vertical group velocity components, $\partial\nu/\partial k$ and $\partial\nu/\partial r$.

$$\text{HGVC}_{\text{CDS-2}} = \frac{\partial\nu_{\text{CDS-2}}}{\partial k} = \frac{f\lambda^2}{B}\frac{\sin k\Delta x}{\Delta x/2}\left(\frac{\sin r\Delta\zeta}{\Delta\zeta}\right)^{-2}, \quad (10)$$

$$\text{VGVC}_{\text{CDS-2}} = \frac{\partial\nu_{\text{CDS-2}}}{\partial r} = -\frac{2f\lambda^2}{B}\left[\frac{\sin(k\Delta x/2)}{\Delta x/2}\right]^2 \times\left(\frac{\sin r\Delta\zeta}{\Delta\zeta}\right)^{-3}\cos r\Delta\zeta. \quad (11)$$

It is obvious that due to the $\cos r\Delta\zeta$ factor in (11) the sign of the $\text{VGVC}_{\text{CDS-2}}$ is wrong (positive) compared to the differential case (5), for the interval

$$\pi/2 < r\Delta\zeta \leqslant \pi, \quad \text{or for} \quad 4\Delta\zeta > L_\zeta \geqslant 2\Delta\zeta. \quad (11')$$

Comparing the computational dispersion characteristics (9)–(11) for the system (1) with the CDS-2 with those of the differential case (3)–(5), we see that the difference between them grows as the smaller resolvable vertical wavelengths are approached. Most importantly, the sign of the VGVC for the CDS-2 is wrong according to (11′) for the resolvable vertical wavelengths smaller than $4\Delta\zeta$.

Let us consider first whether it is possible to improve the situation by using the higher-order scheme for vertical approximation.

b. *The higher-(fourth) order vertical approximation with a regular grid*

Let us derive now the dispersion characteristics for the higher-(fourth) order vertical approximation scheme, or the CDS-4, for the same regular grid considered in section 3a. Namely, applying the fourth-order vertical differencing operator $F^{(4)}_\zeta$ in the form

$$F^{(4)}_\zeta = \frac{4}{3}\bar{F}^\zeta_\zeta - \frac{1}{3}\bar{F}^{2\zeta}_{2\zeta}$$

$$= \frac{4}{3}\frac{1}{2\Delta\zeta}[F(\zeta+\Delta\zeta) - F(\zeta-\Delta\zeta)]$$

$$- \frac{1}{3}\frac{1}{4\Delta\zeta}[F(\zeta+2\Delta\zeta) - F(\zeta-2\Delta\zeta)] \quad (12)$$

for calculating vertical derivatives in the system (6) yields

$$\nu_{\text{CDS-4}} = fC, \quad \text{where} \quad C = \left\{1 + 2\lambda^2\left[\frac{\sin(k\Delta x/2)}{\Delta x/2}\right]^2\left(\frac{\sin r\Delta\zeta}{\Delta\zeta}\right)^{-2}\left(\frac{1}{3}\right)^{-2}(4-\cos r\Delta\zeta)^{-2}\right\}^{1/2}, \quad (13)$$

$$\text{HGVC}_{\text{CDS-4}} = \frac{\partial\nu_{\text{CDS-4}}}{\partial k} = \frac{f\lambda^2}{C}\frac{\sin k\Delta x}{\Delta x/2}\left[\left(\frac{\sin r\Delta\zeta}{\Delta\zeta}\right)\left(\frac{1}{3}\right)(4-\cos r\Delta\zeta)\right]^{-2}, \quad (14)$$

$$\text{VGVC}_{\text{CDS-4}} = \frac{\partial\nu_{\text{CDS-4}}}{\partial r} = -\frac{2f\lambda^2}{C}\left[\frac{\sin(k\Delta x/2)}{\Delta x/2}\right]^2\left(\frac{\sin r\Delta\zeta}{\Delta\zeta}\right)^{-3}\left(\frac{1}{3}\right)^{-2}(4-\cos r\Delta\zeta)^{-3}(4\cos r\Delta\zeta - \cos 2r\Delta\zeta). \quad (15)$$

The sign of the $\text{VGVC}_{\text{CDS-4}}$ (15) depends on the sign of the expression $(4\cos r\Delta\zeta - \cos 2r\Delta\zeta)$ and is wrong (positive) for the approximate interval

$$\approx \frac{4}{7}\pi < r\Delta\zeta \leqslant \pi, \quad \text{or for} \quad \approx 3.5\Delta\zeta > L_\zeta \geqslant 2\Delta\zeta, \tag{15'}$$

which is slightly smaller than that for the second-order scheme CDS-2 (11′) for which the left limit is $4\Delta\zeta$.

Therefore, the introduction of the higher-order approximation scheme for vertical differencing only slightly improves the situation as regards such an important dispersion characteristic as the range of the appropriate sign of the VGVC. Note that Leslie and Purser (1991) have shown some improvements when applying the higher-order schemes with the unstaggered grid for a semi-Lagrangian formulation. A more detailed discussion of the higher-(fourth) order approximation with different grids will be continued in sections 3h and 4.

c. The Lorenz grid

We will examine below the possibility of improving computational dispersion properties when using vertically staggered grids.

Let us consider first the vertically staggered Lorenz grid presented in (Fig. 1). The CDS-2 with the L grid for the system (1) has the form

$$\begin{aligned} \bar{u}^t_t + \bar{\phi}^\zeta_x - fv &= 0, \\ \bar{v}^t_t + \bar{\phi}^\zeta_y + fu &= 0, \\ \bar{\phi}^{t\zeta}_\zeta + c^2\Omega &= 0, \\ u_x + v_y + \Omega_\zeta &= 0. \end{aligned} \tag{16}$$

For the system (16) we have the following dispersion characteristics:

$$\nu_L = fD, \quad \text{where} \quad D = \left\{1 + 2\lambda^2\left[\frac{\sin(k\Delta x/2)}{\Delta x/2}\right]^2\left[\frac{\sin(r\Delta\zeta/2)}{\Delta\zeta/2}\right]^{-2}\right\}^{1/2}, \tag{17}$$

$$\mathrm{HGVC}_L = \frac{\partial\nu_L}{\partial k} = \frac{f\lambda^2}{D}\frac{\sin k\Delta x}{\Delta x/2}\left[\frac{\sin(r\Delta\zeta/2)}{\Delta\zeta/2}\right]^{-2}, \tag{18}$$

$$\mathrm{VGVC}_L = \frac{\partial\nu_L}{\partial r} = -\frac{2f\lambda^2}{D}\left[\frac{\sin(k\Delta x/2)}{\Delta x/2}\right]^2\left[\frac{\sin(r\Delta\zeta/2)}{\Delta\zeta/2}\right]^{-3}\cos\left(\frac{r\Delta\zeta}{2}\right). \tag{19}$$

Comparing expressions (17)–(19) with those of the unstaggered grid (9)–(11) yields to the conclusion that the dispersion characteristics for the L grid are the same as for the unstaggered grid with the CDS-2 if the vertical increment $\Delta\zeta$ is replaced by the half increment $\Delta\zeta/2$. Therefore, the computational dispersion characteristics for the L grid correspond precisely to those of the regular (unstaggered) grid with twice the vertical resolution.

d. The Charney–Phillips grid

For the vertically staggered CP grid (Fig. 1) the CDS-2 for the system (1) has the following form:

$$\begin{aligned} \bar{u}^t_t + \phi_x - fv &= 0, \\ \bar{v}^t_t + \phi_y + fu &= 0, \\ \bar{\phi}^t_{t\zeta} + c^2\Omega &= 0, \\ u_x + v_y + \Omega_\zeta &= 0. \end{aligned} \tag{20}$$

The system (20) does not include any vertical averaging and precisely corresponds to the scheme with the regular vertical grid with twice the vertical resolution.

The dispersion characteristics for system (20) are identical to those for the L grid (17)–(19). Therefore, besides having the same advantageous dispersion properties as the L grid, the CP grid is in addition free of the noise generation problem for baroclinic discrete systems as pointed out by Arakawa and Moorthi (1988). All this makes the CP grid at least as attractive a candidate as the L grid for atmospheric models.

e. The time-staggered version of the Lorenz grid

Let us now consider the dispersion properties of the new type of vertical grids, namely, time-vertically staggered grids. The time-vertically staggered version of the L grid, or the LTS grid, is presented in Fig. 1. The time-staggering procedure is defined to have corresponding vertical grids shifting and alternating for adjacent time steps by half a vertical interval. Namely, at two adjacent time steps, t_n and t_{n+1}, the grids have the same vertical distribution of variables as for the L grid but are shifted by $\Delta\zeta/2$. Therefore, for such a grid the vertical distribution of variables repeats itself in one time step.

Note that to avoid possible problems related to calculations at the top and bottom of the vertical integration domain such as treatment of orography, surface flux calculations, height calculation from the hydrostatic equation, and formulation of the upper boundary condition, there is an option of keeping the lower and upper levels the same for both adjacent time steps. To maintain approximately regular vertical resolution, it

is possible to redistribute the levels in the vicinity of lower and upper boundaries.

The CDS for the system (1) when using the LTS grid is as follows:

$$\bar{u}_t^t + \phi_x - f\bar{v}^\zeta = 0,$$
$$\bar{v}_t^t + \phi_y - f\bar{u}^\zeta = 0,$$
$$\bar{\phi}_{t\zeta}^t + c^2\Omega = 0,$$
$$u_x + v_y + \Omega_\zeta = 0, \tag{21}$$

for which

$$\nu_{\mathrm{LTS}} = fE, \quad \text{where} \quad E = \left\{\cos^2\frac{r\Delta\zeta}{2} + 2\lambda^2\left[\frac{\sin(k\Delta x/2)}{\Delta x/2}\right]^2\left[\frac{\sin(r\Delta\zeta/2)}{\Delta\zeta/2}\right]^{-2}\right\}^{1/2}, \tag{22}$$

$$\mathrm{HGVC}_{\mathrm{LTS}} = \frac{\partial\nu_{\mathrm{LTS}}}{\partial k} = \frac{f\lambda^2}{E}\frac{\sin k\Delta x}{\Delta x/2}\left[\frac{\sin(r\Delta\zeta/2)}{\Delta\zeta/2}\right]^{-2}, \tag{23}$$

$$\mathrm{VGVC}_{\mathrm{LTS}} = \frac{\partial\nu_{\mathrm{LTS}}}{\partial r} = -\frac{f}{E}\left\{\frac{\Delta\zeta}{4}\sin r\Delta\zeta + 2\lambda^2\left[\frac{\sin(k\Delta x/2)}{\Delta x/2}\right]^2\left[\frac{\sin(r\Delta\zeta/2)}{\Delta\zeta/2}\right]^{-3}\right\}. \tag{24}$$

Because of the vertical averaging introduced for the Coriolis terms in (21), $\bar{u}^\zeta$ and $\bar{v}^\zeta$, we obtained first terms in (22) and (24) different from those of (17) and (19). However, the appropriate negative sign of the $\mathrm{VGVC}_{\mathrm{LTS}}$ will not be affected by the difference for the resolvable vertical scales $L_\zeta \geq 2\Delta\zeta$ for which $\sin r\Delta\zeta \geq 0$. Moreover, the difference itself is of a second order of magnitude with respect to the small arguments $r\Delta\zeta$ and $\Delta\zeta$; namely, $\cos(r\Delta\zeta/2) \to 1 + O[(r\Delta\zeta)^2]$ and $(\Delta\zeta/4)\sin r\Delta\zeta \to O[r(\Delta\zeta)^2]$. For this case, the dispersion characteristics of the LTS grid (22)–(24) are very close to those for the L and the CP grids (17)–(19).

Generally, there is the additional, unique, useful option provided by a time-staggering procedure; namely, *for the time-staggered vertical grids it is always possible to replace a vertical averaging operator by the corresponding two-time-level averaging operator* $\tilde{F}^t$ (7). Using the option for the Coriolis terms in (21) yields

$$\bar{u}_t^t + \phi_x - f\tilde{v}^t = 0,$$
$$\bar{v}_t^t + \phi_y + f\tilde{u}^t = 0,$$
$$\bar{\phi}_{t\zeta}^t + c^2\Omega = 0,$$
$$u_x + v_y + \Omega_\zeta = 0. \tag{25}$$

Note that although the two equations of motion in (25) contain the time-averaging operators for the Coriolis terms, the future wind components, u^{n+1} and v^{n+1}, in this case can be calculated explicitly because the equations are linear in respect to u^{n+1} and v^{n+1}. For system (25) the dispersion characteristics are identical to those for the L grid (17)–(19) when $\nu\Delta t \to 0$ and, therefore, correspond to the grid with twice the vertical resolution.

f. The time-staggered version of the Charney–Phillips grid

The time-staggered version of the CP grid, or the CPTS grid, is presented in Fig. 1. The CDS for the grid for the system (1) is as follows:

$$\bar{u}_t^t + \bar{\phi}_x^\zeta - f\bar{v}^\zeta = 0,$$
$$\bar{v}_t^t + \bar{\phi}_y^\zeta + f\bar{u}^\zeta = 0,$$
$$\bar{\phi}_{t\zeta}^t + c^2\bar{\Omega}^\zeta = 0,$$
$$u_x + v_y + \Omega_\zeta = 0. \tag{26}$$

For the system the dispersion characteristics are

$$\nu_{\mathrm{CPTS}} = fG, \quad \text{where} \quad G = \cos\frac{r\Delta\zeta}{2}\left\{1 + 2\lambda^2\left[\frac{\sin(k\Delta x/2)}{\Delta x/2}\right]^2\left[\frac{\sin(r\Delta\zeta/2)}{\Delta\zeta/2}\right]^{-2}\right\}^{1/2}, \tag{27}$$

$$\mathrm{HGVC}_{\mathrm{CPTS}} = \frac{\partial\nu_{\mathrm{CPTS}}}{\partial k} = \frac{f\lambda^2}{G}\frac{\sin k\Delta x}{\Delta x/2}\left[\frac{\tan(r\Delta\zeta/2)}{\Delta\zeta/2}\right]^{-2}, \tag{28}$$

$$\mathrm{VGVC}_{\mathrm{CPTS}} = \frac{\partial\nu_{\mathrm{CPTS}}}{\partial r} = -\frac{f}{G}\left\{\frac{\Delta\zeta}{4}\sin r\Delta\zeta + 2\lambda^2\left[\frac{\sin(k\Delta x/2)}{\Delta x/2}\right]^2\left[\frac{\sin(r\Delta\zeta/2)}{\Delta\zeta/2}\right]^{-3}\cos\frac{r\Delta\zeta}{2}\right\}. \tag{29}$$

These dispersion characteristics of the CPTS grid (27)–(29) are close to those for the LTS grid (22)–(24) and for the L and CP grids (17)–(19) when $r\Delta\zeta$ and/or $\Delta\zeta$ are small.

Using, as in the previous subsection, the additional option provided by the time-staggering procedure, we can replace the vertical averaging operators in system (26) by time averaging operators and obtain the following semi-implicit scheme for the CPTS grid:

$$\begin{aligned} \bar{u}_t^t + \tilde{\phi}_x^t - f\tilde{v}^t &= 0, \\ \bar{v}_t^t + \tilde{\phi}_y^t + f\tilde{u}^t &= 0, \\ \bar{\phi}_{t\zeta}^t + c^2\tilde{\Omega}^t &= 0, \\ u_x + v_y + \Omega_\zeta &= 0. \end{aligned} \tag{30}$$

For the system (30) the dispersion characteristics are identical to those for the L grid (17)–(19) when $\nu\Delta t \to 0$ and also correspond to the grid with twice the vertical resolution.

g. *Staggered grids carrying all velocity components at the same levels*

For all staggered grids considered in the preceding subsections, the vertical velocity Ω and the horizontal velocity components u and v are carried at different levels (Fig. 1). To complete our consideration of all possible vertical grids for the baroclinic system (1), we introduce two more vertically staggered grids, N1 and N2, and their time-vertically staggered versions, N1TS and N2TS, for which all three velocity components, u, v, and Ω, are carried at the same levels (Fig. 2). Finally, we consider also the time-staggered version of the regular (unstaggered) grid or the N3ST grid, for which all variables are carried at the same level (Fig. 2).

Notice that contrary to the Lorenz and Charney–Phillips grids, for example, for the grids carrying all velocity components at the same levels it is difficult to maintain conservation laws or integral constraints for quasigeostrophic flows.

For vertically staggered N1 and N2 grids the corresponding CDSs are as follows:

for the N1 grid,

$$\begin{aligned} \bar{u}_t^t + \phi_x - fv &= 0, \\ \bar{v}_t^t + \phi_y + fu &= 0, \\ \bar{\phi}_{t\zeta}^t + c^2\bar{\Omega}^\zeta &= 0, \\ u_x + v_y + \bar{\Omega}_\zeta^\zeta &= 0, \end{aligned} \tag{31}$$

and for the N2 grid,

$$\begin{aligned} \bar{u}_t^t + \bar{\phi}_x^\zeta - fv &= 0, \\ \bar{v}_t^t + \bar{\phi}_x^\zeta + fu &= 0, \\ \bar{\phi}_{t\zeta}^t + c^2\Omega &= 0, \\ u_x + v_y + \bar{\Omega}_\zeta^\zeta &= 0. \end{aligned} \tag{32}$$

There is a loss of accuracy of vertical approximation, or a decrease of effective vertical resolution, for systems (31) and (32) due to the term $\bar{\Omega}_\zeta^\zeta$ in the continuity equation. For this, the effective vertical resolution is the same as for a regular (nonstaggered) grid (6), compared to term Ω_ζ for all systems with staggered grids considered above, for which the effective vertical resolution is twice as fine. This is an evident drawback of these two vertically staggered grids, N1 and N2.

Let us now consider the CDSs for the time-staggered versions of the N1 and N2 grids, or for the time-vertically staggered N1TS and N2TS grids. Using an option of replacing the vertical averaging operators by the time averaging operators, provided by the time-staggering procedure, yields the following:

for the N1TS grid,

$$\begin{aligned} \bar{u}_t^t + \tilde{\phi}_x^t - f\tilde{v}^t &= 0, \\ \bar{v}_t^t + \tilde{\phi}_y^t + f\tilde{u}^t &= 0, \\ \bar{\phi}_{t\zeta}^t + c^2\Omega &= 0, \\ \tilde{u}_x^t + \tilde{v}_y^t + \Omega_\zeta &= 0, \end{aligned} \tag{33}$$

and for the N2TS grid,

$$\begin{aligned} \bar{u}_t^t + \phi_x - f\tilde{v}^t &= 0, \\ \bar{v}_t^t + \phi_y + f\tilde{u}^t &= 0, \\ \bar{\phi}_{t\zeta}^t + c^2\tilde{\Omega}^t &= 0, \\ \tilde{u}_x^t + \tilde{v}_y^t + \Omega_\zeta &= 0. \end{aligned} \tag{34}$$

System (33) is the CDS with twice the vertical resolution only when combined with the two-time-level semi-implicit time-differencing scheme that suggests an iterative solution (e.g., Bates 1984). System (34) is also the CDS with twice the vertical resolution only when combined with the two-time-level version of the economical explicit scheme introduced in Fox-Rabinovitz (1974). The scheme does not require any iterations but instead requires a certain order of integration for equations of system (34). The two-time-level averaging operators used within the scheme version are consistent with the leapfrog scheme applied for the time-differencing approximation.

For the case, both of the time-vertically staggered N1TS and N2TS grids have dispersion characteristics identical to the expressions (17)–(19) and, therefore, to those of twice the vertical resolution compared to a regular grid.

Finally, for the time-staggered regular (vertically unstaggered) grid, or the N3TS grid (Fig. 2), the CDS for system (1), when using the option (available for the vertical time-staggered grids) of replacing the vertical averaging operators by the corresponding time averaging operators, results in a semi-implicit scheme:

$$\begin{aligned} \bar{u}_t^t + \tilde{\phi}_x^t - f\tilde{v}^t &= 0, \\ \bar{v}_t^t + \tilde{\phi}_y^t + f\tilde{u}^t &= 0, \end{aligned}$$

$$\bar{\phi}^{t}_{t\zeta} + c^2\tilde{\Omega}^{t} = 0,$$

$$u_x + v_y + \tilde{\Omega}^{t}_{\zeta} = 0. \qquad (35)$$

The dispersion characteristics for system (35) again correspond to those of a regular grid with twice the vertical resolution.

Although grids included into this subsection cannot be recommended for use in atmospheric models because of the difficulty of maintaining conservation laws or integral constraints for quasigeostrophic flows, it was shown that the grids that were staggered in time and in the vertical still had advantageous dispersion properties when combined with the appropriate economical explicit or semi-implicit schemes.

h. *Higher-(fourth-) order vertical approximation with staggered grids*

The fourth-order approximation (12) may be applied in the way similar to that of section 3b, to all considered schemes with vertically and time vertically staggered grids. The typical example of the scheme of this kind is equations (20) for the CP grid with twice the effective vertical resolution compared to a regular grid (6). The computational dispersion characteristics for the scheme (20) with the fourth-order vertical approximation (12), or the CP-4 scheme, are identical to those of a regular grid with the CDS-4 (13)–(15) with the argument $r\Delta\zeta$ and the increment $\Delta\zeta$ replaced by $r\Delta\zeta/2$ and $\Delta\zeta/2$, respectively.

The impact of the higher-(fourth) order approximation on computational dispersion properties of staggered grids will be further discussed in section 4. In this case, the sign of the $VGVC_{CP\text{-}4}$ depends on the sign of the expression $4\cos(r\Delta\zeta/2) - \cos r\Delta\zeta$, which is positive for $0 \leqslant r\Delta\zeta \leqslant \pi$, or for all resolvable scales $L \geqslant 2\Delta\zeta$. Therefore, the sign of the $VGVC_{CP\text{-}4}$ is correct (negative) for all resolvable scales as for all staggered grids with twice the vertical effective resolution.

This completes our consideration of all possible vertical grids applicable to atmospheric primitive equation systems using the hydrostatic approximation.

i. *Effective resolution for different vertical grids*

We have already shown that all vertically and time-vertically staggered grids have effectively twice the vertical resolution compared to a regular (unstaggered) grid for the adjustment system (1). However, the time-vertically staggered grids have additional advantage over vertically staggered grids for a full primitive equation system. Namely, the vertical advection and diffusion terms containing first and second vertical derivatives for full baroclinic nonlinear models are also approximated with twice the vertical effective resolution for all time-vertically staggered grids considered above (see Table 1).

TABLE 1. Effective vertical resolution for adjustment, and vertical advection and diffusion terms for different vertical grids.

Regular (unstaggered) grid	Vertically staggered grids (L, CP)	Time-vertically staggered grids (LTS, CPTS, N1TS, N2TS, N3TS)
	Adjustment terms	
$2\Delta\zeta$	$\Delta\zeta$	$\Delta\zeta$
	Vertical advection and diffusion terms	
$2\Delta\zeta$	$2\Delta\zeta$	$\Delta\zeta$

For example, the centered-finite-difference approximations of the vertical advection and diffusion terms, if added to the u-component equation of system (1), will have the following expressions, when using definitions (7), for the regular (unstaggered) grid,

$$\Omega\frac{\partial u}{\partial\zeta} \sim \Omega\bar{u}^{\zeta} \quad \text{and} \quad K\frac{\partial^2 u}{\partial\zeta^2} \sim Ku_{\zeta\zeta}, \qquad (36)$$

and vertically staggered grids,

$$\Omega\frac{\partial u}{\partial\zeta} \sim \bar{\Omega}^{\zeta}\bar{u}^{\zeta} \quad \text{and} \quad K\frac{\partial^2 u}{\partial\zeta^2} \sim Ku_{\zeta\zeta}, \qquad (36')$$

where K is a diffusion coefficient. In contrast to that, for the time-vertically staggered grids, these expressions, when using definitions (7), are

$$\Omega\frac{\partial u}{\partial\zeta} \sim \Omega u_{\zeta} \quad \text{and} \quad K\frac{\partial^2 u}{\partial\zeta^2} \sim K\tilde{u}_{\zeta\zeta}, \qquad (37)$$

which indicates using twice the effective vertical resolution.

Note that for approximation of the vertical diffusion terms here the following stable scheme could be used (Du Fort and Frankel 1953):

$$Ku_{\zeta\zeta} \sim K(u^{n}_{l-1} + u^{n}_{l+1} - u^{n+1}_{l} - u^{n-1}_{l}), \quad \text{and}$$

$$K\tilde{u}_{\zeta\zeta} \sim K(u^{n}_{l-1/2} + u^{n}_{l+1/2} - u^{n+1}_{l} - u^{n-1}_{l}), \qquad (38)$$

where n is the time index (8).

Therefore, whereas vertically staggered grids provide twice the effective vertical resolution for adjustment terms but not for vertical advection and diffusion terms, only time-vertically staggered grids provide uniformly twice the vertical effective resolution for both adjustment and vertical advection and diffusion terms. In other words, the considered time-vertically staggered grids provide a *uniformly doubled effective vertical resolution* for the full baroclinic model system.

4. Discussion

We will compare in this section the dispersion characteristics derived in the section 3 for the vertical grids considered.

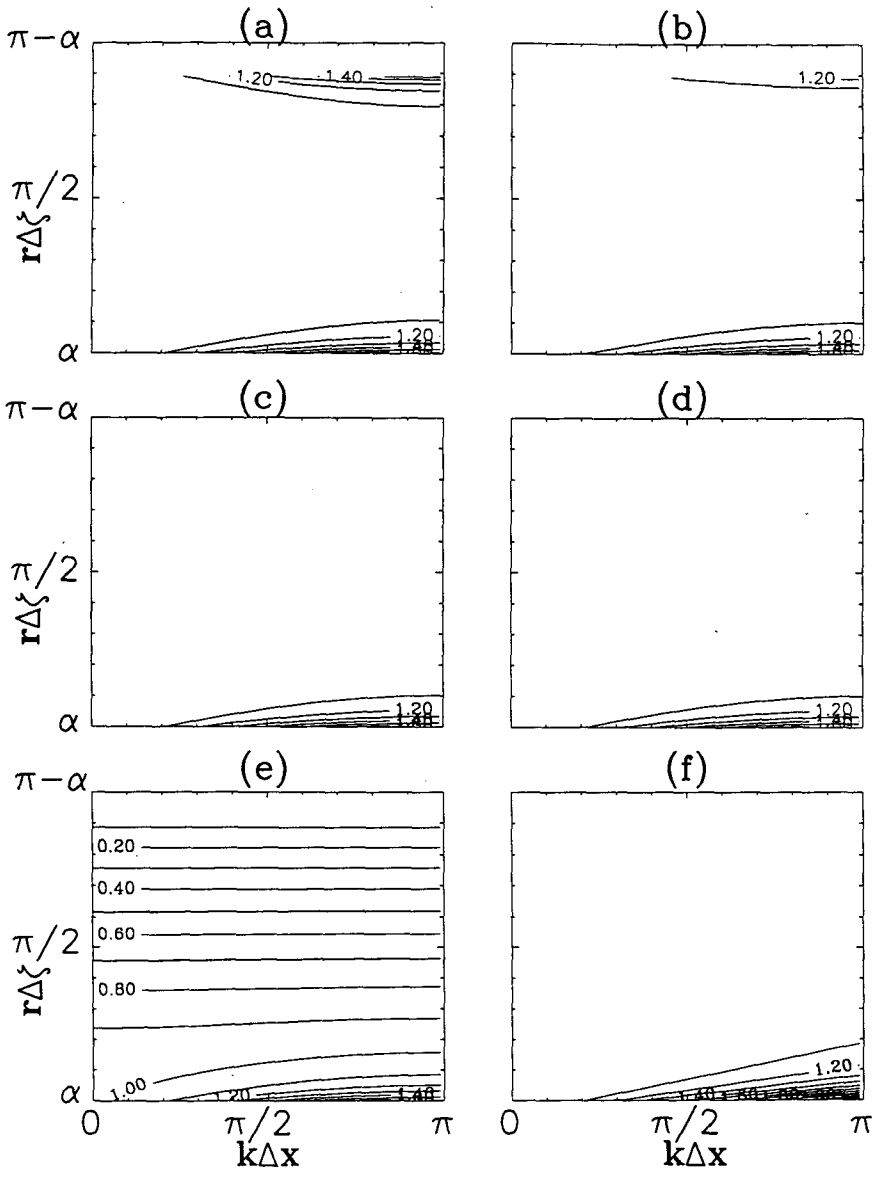

FIG. 3. Frequencies for the regular (unstaggered) vertical grid with (a) the CDS-2 and (b) the CDS-4; (c) for the vertically staggered L and CP grids and all time-vertically staggered grids with the two-time-level versions of semi-implicit or economical explicit schemes; (d) the CP grid with the CDS-4, or the CP-4 grid; (e) the time-vertically staggered CPTS grid; and (f) the differential case. The Brunt–Väisälä oscillation frequency is α. The contour interval is 0.2. (The scale factor for frequency is 10^4 s^{-1}.)

Let us first consider the computational dispersion properties of different vertically staggered grids presented in Figs. 3–5 and compare them with the ones of the differential case, and with each other. For the regular (unstaggered) vertical grid, both the frequency and the HGVC (Figs. 3a and 4a) contain erroneous pattern features for $\pi \geq r\Delta\zeta > \pi/2$, or for the vertical scales $2\Delta\zeta \leq L_\zeta < 4\Delta\zeta$. Most importantly, the VGVC for the case (Fig. 5a) has the wrong (positive) sign for the aforementioned vertical scale range. This suggests that for this range an appropriate filtering should be applied to control the noise when using a regular vertical grid with the CDS-2.

Application of the higher-(fourth) order CDS-4 with the regular vertical grid (Figs. 3b, 4b, and 5b) provides some improvement of all computational dispersion characteristics compared to those for the CDS-2. The range of the wrong (positive) sign of the $\mathrm{VGVC}_{\mathrm{CDS\text{-}4}}$ (15) and the corresponding

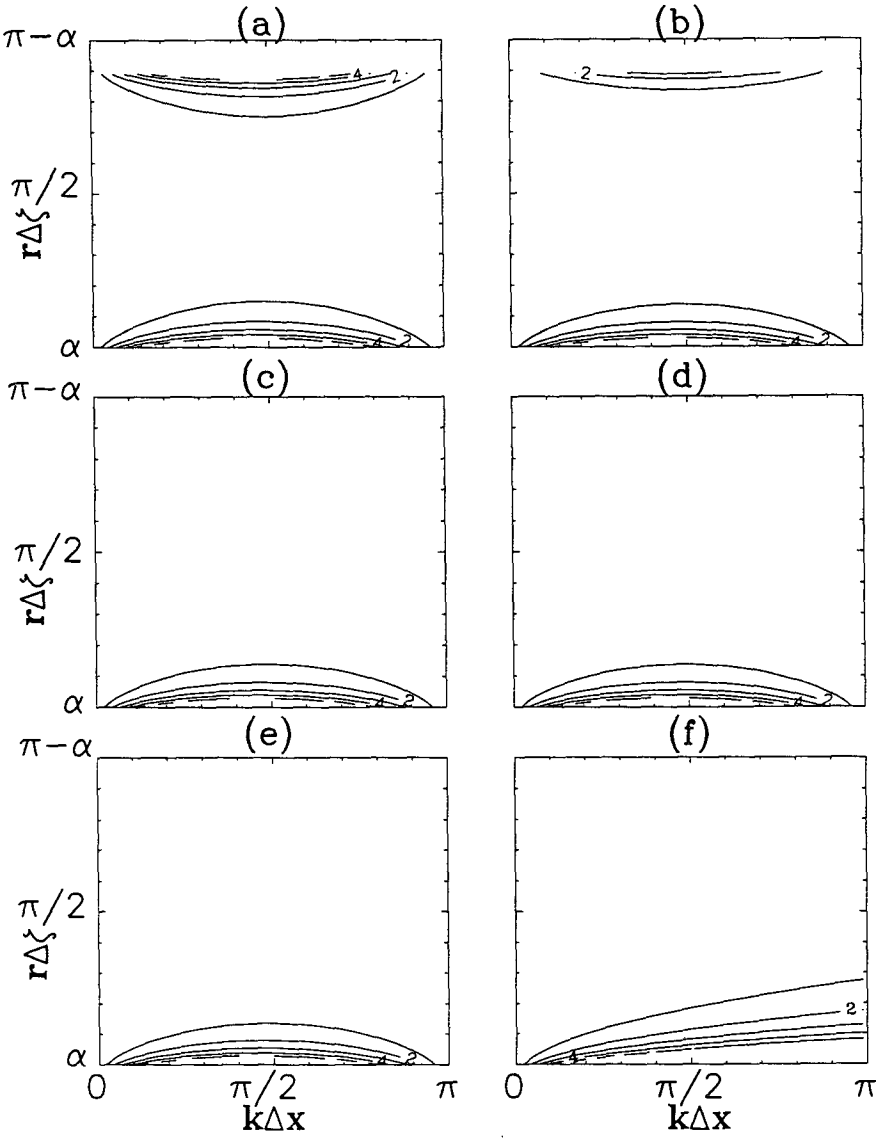

FIG. 4. The horizontal group velocity components, or the HGVCs, for the same grids as in Fig. 3. The contour interval is 1. (The scale factor for the HGVCs is 10 m s^{-1}.)

range of filtration are only slightly smaller, according to (15′), than for the $VGVC_{CDS-2}$ (11′), which may be concluded by comparing Figs. 5b and 5a.

The same characteristics for vertically and time-vertically staggered grids (Figs. 3c, 4c, and 5c) (the latter only when combined with the corresponding semi-implicit or economic explicit scheme) are significantly better, corresponding to a regular grid with twice the vertical resolution. Most importantly, the sign of the VGVCs for the grids is correct for all resolvable vertical scales $L_\zeta \geqslant 2\Delta\zeta$.

To estimate quantitatively in more detail and further compare the dispersion properties of different vertical grids, the relative differences between computational dispersion characteristics for considered vertical grids and those of the differential case are calculated and shown in Figs. 6–8. By the relative differences R, or relative errors, we mean the differences D, divided or normalized by the corresponding computational dispersion characteristic value C_j^{diff} for the differential case (4)–(5): namely,

$$R_j^i = \frac{D_j^i}{C_j^{\text{diff}}} = \frac{C_j^i - C_j^{\text{diff}}}{C_j^{\text{diff}}},$$

where the upper index i stands for a grid and the lower index j for a computational dispersion characteristic (frequency, the HGVC or the VGVC). For the regular vertical grid with the CDS-2 and the CDS-4 (Figs. 6a,b,

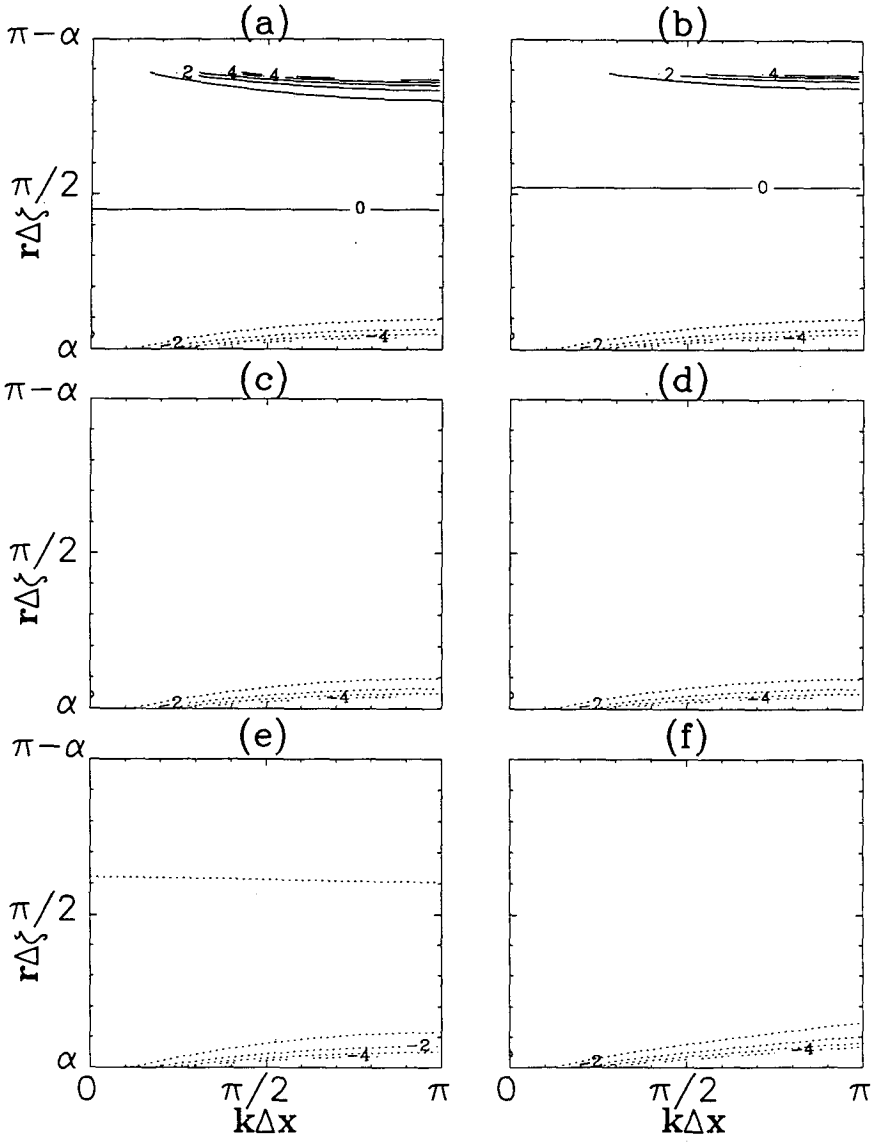

FIG. 5. The vertical group velocity components, or the VGVCs, for the same grids as in Fig. 3. The contour interval is 1.

Figs. 7a,b, and Figs. 8a,b) there is an area with large relative errors for small vertical scales (the upper part of the figures). The application of a vertical filtering procedure in this scale range is desirable. The relative errors are slightly smaller for the CDS-4.

The relative errors for the vertically and time-vertically staggered grids with the CDS-2 and for the vertically staggered CP grid with the CDS-4, or the CP-4 grid (Figs. 6c,d, Figs. 7c,d, and Figs. 8c,d) are small for the small vertical scales due to the fact that they have twice the effective vertical resolution compared to that of the regular vertical grid. Moreover, the CP-4 grid has definitely smaller relative errors for the large horizontal and small vertical scale range (left upper corner of the figures). The improvement is rather noticeable for the HGVC and the VGVC (Figs. 7c,d and Figs. 8c,d). Therefore, the application of the higher-order approximation in the vertical when using vertically and time-vertically staggered grids may be appropriate mostly for the better representation of the aforementioned scale range.

For comparison we present the relative errors for the time-vertically staggered grid (Figs. 6e, 7e, and 8e) for which vertical averaging operators are not replaced by the corresponding time averaging operators (27)–(29). The relative errors for the case are worse especially for frequency and the VGVC compared to those presented in Figs. 6c,d, Figs. 7c,d, and Figs. 8c,d. It is worth mentioning that even for the vertical grids with the best computational dispersion properties the

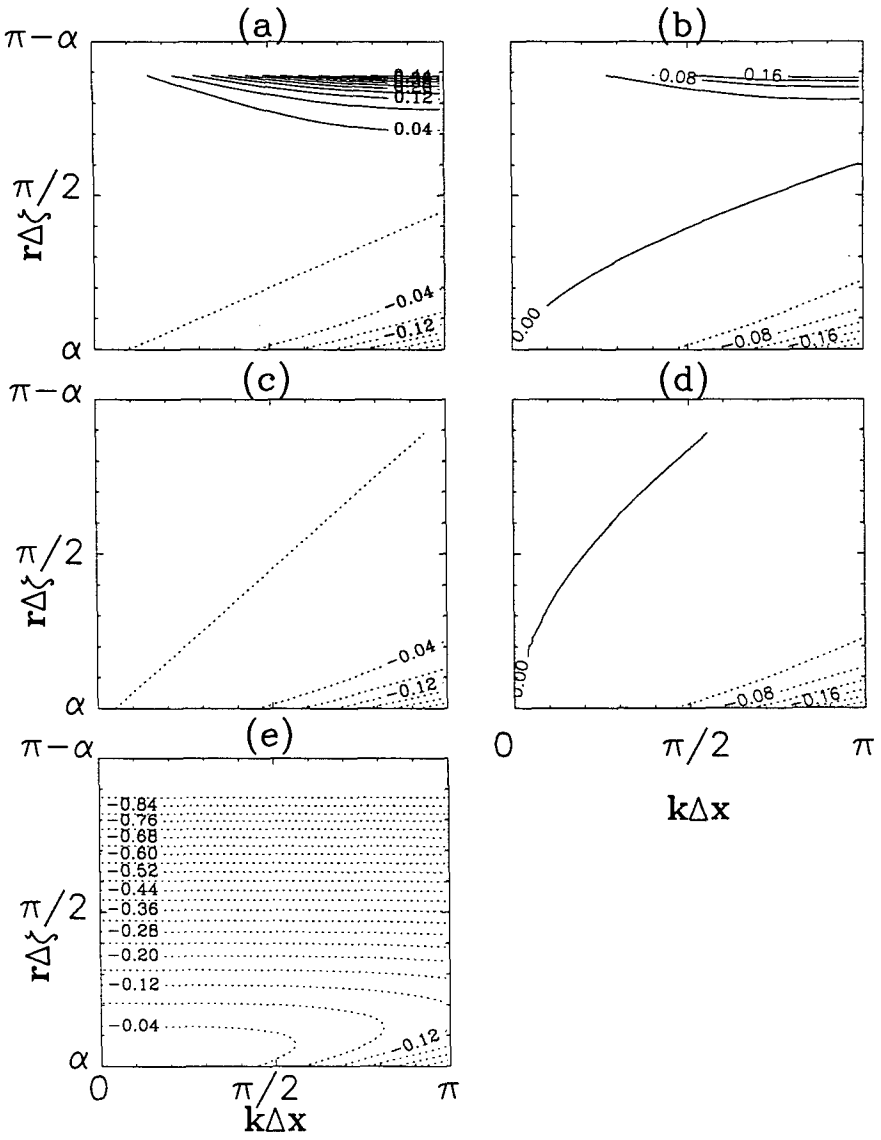

FIG. 6. Relative errors R for frequencies for the same grids as in Fig. 3 except for the differential case. The contour interval is 0.04.

VGVCs are underestimated for all resolvable scales (Figs. 8c,d).

5. Conclusions

Our concluding remarks and recommendations can be summarized as follows.

1) Computational dispersion properties for practically all possible vertically and time-vertically staggered grids applicable for centered-difference approximations of primitive equation atmospheric models have been considered. The grids are computationally efficient due to enhanced effective vertical resolution doubled through staggering, as compared to that of a regular (unstaggered) vertical grid. In other words, for all the best staggered grids considered, the computational dispersion properties are either similar to or identical with those of a regular grid having *twice the vertical resolution* for a baroclinic gravity–inertial wave or adjustment system.

2) Among vertically staggered grids, the Charney–Phillips (1953) grid and the Lorenz (1960) grid have advantageous computational dispersion and other properties. Moreover, as pointed out by Arakawa and Moorthi (1988), the Charney–Phillips grid in contrast to the Lorenz grid does not generate noise for baroclinic discrete systems. All this deserves to draw more attention of atmospheric modelers to the possibility of *using the Charney–Phil-*

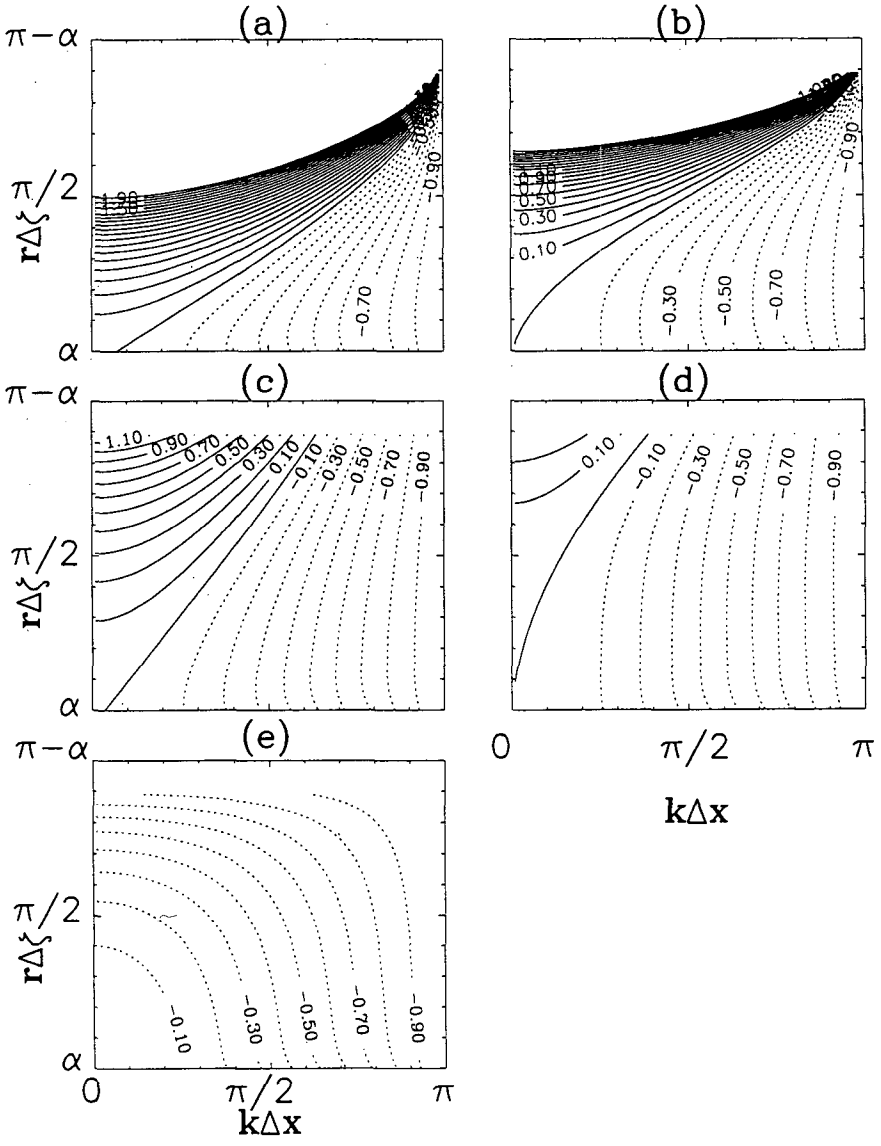

FIG. 7. Relative errors R for the horizontal group velocity components, or the HGVCs, for the same grids as in Fig. 6. The contour interval is 0.1. Contours with $R > 2$ are not shown.

lips grid as widely as the currently most popular Lorenz grid.

3) Vertical group velocity components for all vertically and time-vertically staggered grids have the appropriate sign for all resolvable scales $L \geq 2\Delta\zeta$, whereas for a regular (unstaggered) vertical grid the sign is wrong for the scales $2\Delta\zeta \leq L < 4\Delta\zeta$.

4) For time-centered differencing schemes with time-vertically staggered grids, all *vertical averaging operators may be replaced by time-averaging operators* resulting in either economical explicit or semi-implicit schemes. For this case, the grids have the same advantageous computational dispersion properties as the vertically staggered Lorenz and Charney–Phillips grids.

5) In addition to that, the time-vertically staggered grids have twice the effective vertical resolution for approximation of first and second vertical derivatives in vertical advection and diffusion terms as compared not only with a regular (unstaggered) vertical grid but also with vertically staggered grids. Therefore, the use of time-vertically staggered grids provides a *uniform approximation with twice the effective vertical resolution for all terms* of primitive equation models.

6) The introduction of higher-(fourth) order vertical approximation for a regular grid and for all vertically and time-vertically staggered grids results in a relatively moderate overall improvement of computational dispersion properties. Nevertheless, the

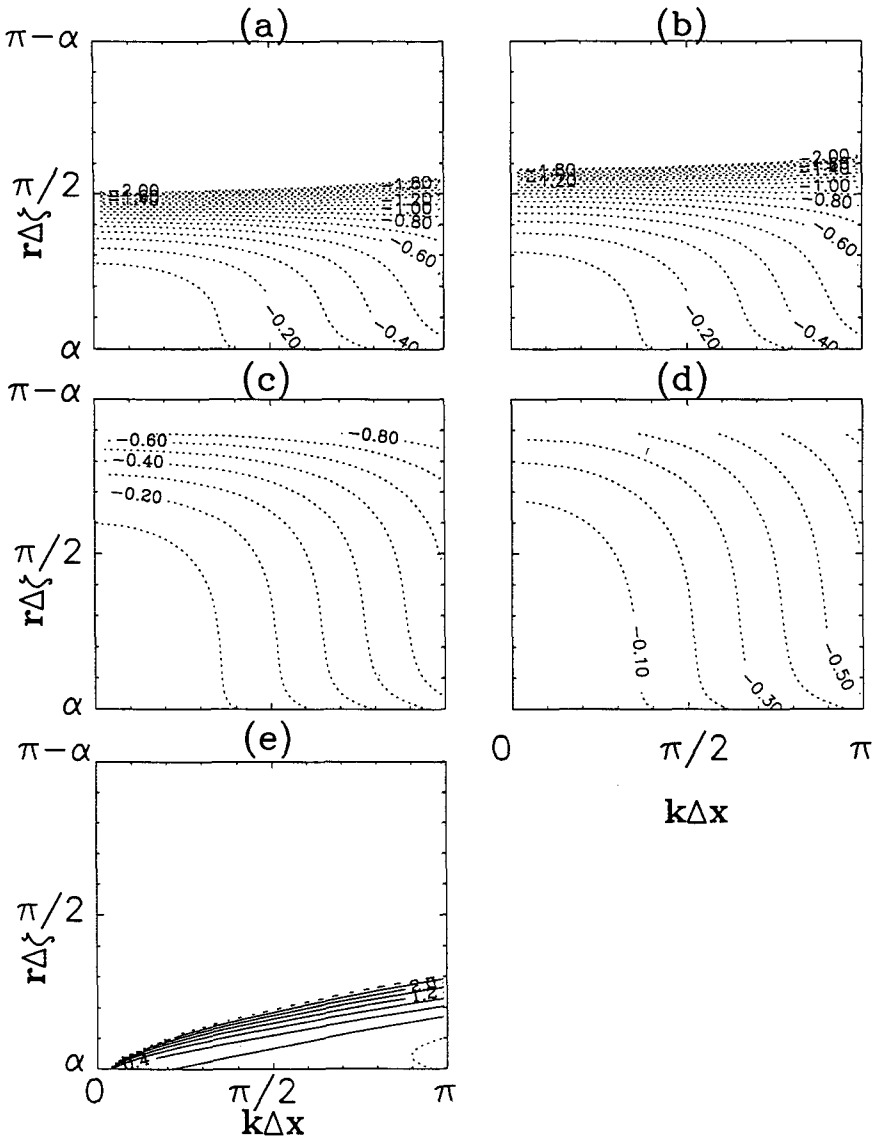

FIG. 8. Relative errors R for the vertical group velocity components, or the VGVCs, for the same grids as in Fig. 6. The contour interval for (a)–(d) is 0.1, and for (e) 0.4. Contours with $R < -2$ are not shown.

use of the higher-order vertical approximation for all these vertical grids results in the rather noticeable decrease of relative errors mostly for the small vertical and large horizontal scale range, especially for the HGVC and VGVC. It is worth mentioning that it is rather easy to implement at least outside the vertical boundaries.

Acknowledgments. I would like to thank Dr. J. R. Bates for his valuable comments, Mr. R. Govindaraju for programming support, and Ms. Q. Philpot for typing the manuscript. The research was supported by the NASA Grant 578-41-25-20.

REFERENCES

Arakawa, A., 1984: Vertical differencing of filtered models. *Numerical Methods for Weather Prediction. Seminar,* Reading, England, European Centre for Medium-Range Forecasting, 183–206.

——, and M. S. Suarez, 1983: Vertical differencing of the primitive equations in sigma coordinates. *Mon. Wea. Rev.,* **111,** 34–45.

——, and S. Moorthi, 1988: Baroclinic instability in vertically discrete systems. *J. Atmos. Sci.,* **45,** 1688–1707.

Bates, J. R., 1984: An efficient semi-Lagrangian and alternating direction implicit method for integrating the shallow water equations. *Mon. Wea. Rev.,* **112,** 2033–2047.

Brown, J. A., and K. Campana, 1978: An economical time-differencing system for numerical weather prediction. *Mon. Wea. Rev.,* **106,** 1125–1135.

Charney, J. C., and N. A. Phillips, 1953: Numerical integration of the quasi-geostrophic equations for barotropic and simple baroclinic flows. *J. Meteor.*, **10,** 17–29.

Du Fort, E. C., and S. P. Frankel, 1953: Stability conditions in the numerical treatment of parabolic differential equations. *Mathematical Tables and Other Aids to Computation,* **7,** 135–152.

Eliassen, A., 1956: A procedure for numerical integration of the primitive equations of the two-parameter model of the atmosphere. Science Report No. 4, Department of Meteorology, University of California, Los Angeles, 56 pp.

Fox-Rabinovitz, M. S., 1974: Economical explicit and semi-implicit integration schemes for forecast equations. *Soviet Meteor. Gidrol.,* **11,** 11–19 (in Russian).

——, 1988: On dispersion properties of some regular and irregular grids used in atmospheric models. *Proc. of the Eighth Conf. on Numerical Weather Prediction,* Baltimore, MD, Amer. Meteor. Soc., 784–789.

——, 1991a: Computational dispersion properties of horizontal staggered grids for atmospheric and ocean models. *Mon. Wea. Rev.,* **119,** 1624–1639.

——, 1991b: Computational dispersion properties of vertical grids for atmospheric models. *Proc. 13th World Congress on Computational and Applied Mathematics,* Dublin, Ireland, International Association for Mathematics and Computers in Simulation, 579–580.

Grotjahn, R., and J. J. O'Brian, 1976: Some inaccuracies in finite differencing hyperbolic equations. *Mon. Wea. Rev.,* **104,** 180–194.

Leslie, L. M., and R. J. Purser, 1991: High-order numerics in an unstaggered three-dimensional time-split semi-Lagrangian forecast model. *Mon. Wea. Rev.,* **119,** 1612–1623.

Lorenz, E. N., 1960: Energy and numerical weather prediction. *Tellus,* **12,** 364–373.

Mesinger, F., and A. Arakawa, 1976: Numerical methods used in atmospheric models. WMO/ICSU Joint Organizing Committee, GARP Publ. Series, 64 pp.

Neta, B., and R. T. Williams, 1986: Stability and phase speed for various finite element formulations of the advection equation. *Comput. Fluids,* **14,** 393–410.

——, and I. M. Navon, 1989: Analysis of the Turkel–Zwas scheme for the shallow-water equations. *J. Comput. Phys.,* **81,** 277–299.

——, and R. T. Williams, 1989a: Rossby wave frequencies and group velocities for finite element and finite difference approximations to the vorticity-divergence and the primitive forms of the shallow water equations. *Mon. Wea. Rev.,* **117,** 1439–1457.

——, and ——, 1989b: A comparative study of finite elements and finite differences for weather prediction. *Proc. of the Fifth Int. Symp. on Numerical Mech. Eng.,* European Assoc. Mech. Eng., Lausanne, Switzerland, 659–669.

Roache, P. J., 1976: *Computational Fluid Dynamics.* Hermosa Publ., 446 pp.

Robert, A., 1969: The integration of the spectral model of the atmosphere by the implicit method. *Proc. of the WMO/IUGG Symp. on NWP,* Tokyo, Japan Meteorological Agency, 19–24.

Schoenstadt, A. L., 1980: A transfer function analysis of numerical schemes used to simulate geostrophic adjustment. *Mon. Wea. Rev.,* **108,** 1248–1259.

Shuman, F. G., 1971: Resuscitation of an integration procedure. NMC Office Note 54, 55 pp.

Tokioka, T., 1978: Some considerations on vertical differencing. *J. Meteor. Soc. Japan,* **56,** 98–111.

Trefethen, L., 1982: Group velocity in finite-difference schemes. *SIAM Rev.,* **24,** 113–136.

Vichnevetsky, R., and J. B. Bowles, 1982: *Fourier Analysis of Numerical Approximation of Hyperbolic Equations.* SIAM, 140 pp.

Wajsowicz, R. C., 1986: Free planetary waves in finite-difference numerical methods. *J. Phys. Oceanogr.,* **16,** 773–789.